



City Research Online

City, University of London Institutional Repository

Citation: Scott, R., Vidakovic, M., Chikermame, S., McKinley, B. ORCID: 0000-0001-6641-5100, Sun, T. ORCID: 0000-0003-3861-8933, Banerji, P. and Grattan, K. T. V. ORCID: 0000-0003-2250-3832 (2019). Encapsulation of Fiber Optic Sensors in 3-D Printed Packages for use in Civil Engineering Applications: A Preliminary Study. *Sensors*, 19(7), 1689.. doi: 10.3390/s19071689

This is the accepted version of the paper.

This version of the publication may differ from the final published version.

Permanent repository link: <https://openaccess.city.ac.uk/id/eprint/21983/>

Link to published version: <http://dx.doi.org/10.3390/s19071689>

Copyright: City Research Online aims to make research outputs of City, University of London available to a wider audience. Copyright and Moral Rights remain with the author(s) and/or copyright holders. URLs from City Research Online may be freely distributed and linked to.

Reuse: Copies of full items can be used for personal research or study, educational, or not-for-profit purposes without prior permission or charge. Provided that the authors, title and full bibliographic details are credited, a hyperlink and/or URL is given for the original metadata page and the content is not changed in any way.

City Research Online:

<http://openaccess.city.ac.uk/>

publications@city.ac.uk

1 *Type of the Paper: Article*

2 **Encapsulation of Fiber Optic Sensors in 3-D Printed** 3 **Packages for use in Civil Engineering Applications: A** 4 **Preliminary Study**

5 **Richard Scott**^{1*}, **Miodrag Vidakovic**¹, **Sanjay Chikermane**², **Brett McKinley**¹, **Tong Sun**¹,
6 **Pradipta Banerji**², and **Kenneth Grattan**¹

7 ¹ School of Mathematics, Computer Science & Engineering, City, University of London

8 ² Department of Civil Engineering, Indian Institute of Technology Roorkee

9 * Correspondence: richard.scott.1@city.ac.uk

10 Received: date; Accepted: date; Published: date

11 **Abstract:** Fiber optic sensors have considerable potential for measuring strains in the challenging
12 environment posed by today's civil engineering applications. Their long-term reliability and
13 stability are particularly important attributes for assessing, with confidence, effects such as cracking
14 and response to normal (and abnormal) loads. However, given the fragile nature of the bare fiber,
15 the sensors must be packaged to achieve adequate robustness but the resulting increased cost of
16 installation can frequently limit the number of sensors which can be installed or their use may have
17 to be ruled out altogether due to these financial constraints. There is thus potential for the
18 development of a more affordable type of packaging and this paper describes work undertaken to
19 produce a cost-effective and easy-to-use technique for encapsulating fiber optic sensors in resin,
20 taking advantage of 3D printing techniques which are widely available and low-cost. This
21 approach can be used to produce a robust, inexpensive packaged sensor system which is seen as
22 being suitable to be extended to a wider range of uses including installation in concrete structures
23 prior to casting. To evaluate this approach, several such 3-D printed package types and geometries
24 are described and their behaviour is assessed from a programme of laboratory trials, the results from
25 which are presented in the paper. This proof-of-concept testing has demonstrated the considerable
26 potential which 3D printed packages have and the scope for further development and consequent
27 use in civil engineering applications. Areas showing promise and potential, which have been
28 identified from the work undertaken, are discussed.

29 **Keywords:** fiber optic sensor; encapsulation; 3D printing; civil engineering; strain measurement
30

31 **1. Introduction**

32 There is an ongoing need to measure strains in reinforced concrete structures both in the
33 laboratory and in the field. The former is mainly concerned with tests on structural elements such
34 as beams, columns and slabs whilst the latter often involves monitoring full scale structures over
35 extended time periods. Materials involved include concrete (both reinforced and prestressed,
36 *in-situ* and precast), steel, and timber. Concrete is highly alkaline and thus presents a harsh
37 environment for any type of sensor and this, together with the rigors of sensor installation and the

38 concrete casting process, means that sensors for concrete must be designed to be particularly robust
 39 and thus reliable, if they are to function correctly over long periods.

40 There are, potentially, many situations where optical fiber sensors could be used successfully in
 41 civil engineering applications because they are immune, or, at least, relatively immune when
 42 compared with other sensor types, to electromagnetic interference and moisture ingress. They also
 43 have the advantage of being small, compact and lightweight and have attracted considerable
 44 research interest in recent years [1-6]. Fiber Bragg Grating (FBG) sensors have been used
 45 successfully in a wide variety of civil engineering applications [7-13] but they are fragile and thus
 46 must be correctly packaged (i.e. encapsulated) in a way that is tailored to that environment to resist
 47 the effects of climate and usage, if they are to achieve the required level of robustness demanded in
 48 civil engineering environments. Also, they must be suitable for both mounting on the surface of a
 49 structure after construction and, in the case of reinforced/prestressed concrete structures, for
 50 inclusion in the structure prior to concreting. It is important to keep in mind the needs of practicing
 51 civil engineers – the end users – when developing a sensor system for field use since this is a far less
 52 controlled environment when compared to that found in the laboratory.

53 An in-fiber FBG is formed from a periodic modulation of the refractive index of the core of a
 54 photosensitive fibre where the modulation of the refractive index is induced by UV light from a laser
 55 source. The periodic modulation acts as a filter reflecting one wavelength, the Bragg wavelength
 56 (λ), which is expressed by the following formula [14]:

$$57 \quad \lambda = 2n_e\Lambda \quad (1)$$

58 where n_e is the effective refractive index and Λ is the period of the grating. Both strain and
 59 temperature changes will induce a shift of the Bragg wavelength, which can be modelled by the
 60 following equation:

$$61 \quad \Delta\lambda = S_{strain}\Delta\varepsilon + S_T\Delta T \quad (2)$$

62 where S_{strain} and S_T are the strain and temperature sensitivities, respectively and $\Delta\varepsilon$ and ΔT are the
 63 strain and temperature variations respectively. Equation 2 highlights the sensor temperature
 64 dependence associated with the strain measurement, particularly as S_T is considerably larger than
 65 S_{strain} . To have a meaningful determination of the actual (i.e. mechanical) strain, it is necessary to
 66 have an accurate value of the temperature in the vicinity of the FBG.

67 Commercial sensors are readily available for civil engineering applications and a model used
 68 by the authors is shown in Figure 1. It contains two FBGs, one measuring total (i.e. mechanical plus
 69 temperature) strain and the other measuring temperature strain, thus allowing the mechanical strain
 70 to be easily calculated. In a recent illustration of the use of *packaged* sensors for civil
 71 engineering-based strain measurement, six of these sensors were surface mounted by the authors on
 72 the walls of

73



Figure 1. Commercial optical fibre sensor

74 an existing prestressed concrete box girder railway bridge in Mumbai (Figures 2 and 3) for
 75 monitoring the effects of passing trains [15] and sensors have recently been cast into a railway

76 viaduct currently under construction, also in Mumbai (Figures 4 and 5). Unfortunately, the extent
 77 of these
 78



Figure 2. Mumbai railway bridge



Figure 3. Sensors on side wall

79



Figure 4. Mumbai railway viaduct



Figure 5. Sensors on reinforcement cage

80 installations to monitor the bridge widely has been severely constrained by the high price of the
 81 sensors as each cost several hundred US dollars and for a full assessment of a structure of this size,
 82 many hundreds would be needed. This problem can be overcome with more inexpensive devices
 83 and there is a potential market for a reliable, robust, *low cost*, packaged optical fiber sensor that can
 84 be used in this sort of environment, and this paper reports work to date by the authors to develop
 85 such a product.

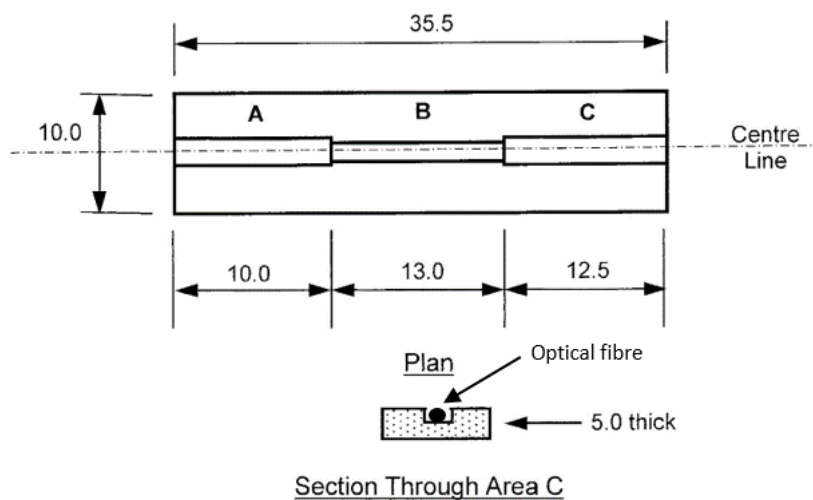
86 Experience gained by the authors from their prior field work in India indicated that for a
 87 package to be successful it must be affordable, robust and durable, yet easy to produce in a range of
 88 geometries. The completed sensor also had to produce high quality, repeatable measurements, be
 89 suitable for surface mounting and also be able to withstand the harsh treatment that comes with
 90 being cast into concrete.

91 Over the last few years there have been considerable advances in the use of 3D printing
 92 techniques with both the hardware and software becoming much more affordable and this forms the
 93 basis of the low-cost sensor discussed. Since both were already available to the authors, a
 94 promising way forward that was identified was to fabricate a suitable packaging that was
 95 compatible with the fiber optic itself using 3D printing techniques. The work built on an initial trial
 96 carried out by the authors that was deemed sufficiently encouraging [16] to warrant the further
 97 work reported in this paper, through a collaboration between City, University of London, and the
 98 Indian Institute of Technology Roorkee.

99 2. Materials and Methods

100 An approach that was both simple and robust was the basis for the design, where initially two
 101 similar open-top packages, as illustrated schematically in Figure 6, were designed with the use of the
 102 software package, *SolidWorks*. (The package was printed first followed by installation of the optical

103 fiber as described below). Standard photopolymer resin was chosen for the fabrication process of
 104 the package, supplied by *Formlabs*. It is a high-resolution resin that ensures both high strength and
 105 high precision of the 3D printed parts, with a Young's modulus of 1.7 GPa. Further, *formlabs Pre*
 106 *Form* software was used to drive a *formlabs 1+* 3D printer after the model designed in *SolidWorks* was
 107 loaded. After 3D printing was completed, the samples were removed from the building platform
 108 and carefully rinsed in isopropyl alcohol (IPA). In order to achieve higher strength of the sample,
 109 all samples were post-cured under a UV (405 nm) lamp for 2 hours. After completion of the
 110 fabrication process, two 5 mm long FBGs were installed in each package, the one in the center of
 111 Section B being glued to the package with Duralco 4525-IP for strain measurement and the other free
 112 (i.e. not glued) in Section C for temperature measurement, both being multiplexed on a single fibre.
 113 The cable leading to the interrogator exited the package along Section A (see Figure 6) and
 114 protection of the strain FBG was achieved by filling Section B with Duralco adhesive. The
 115 temperature FBG was allowed to *float* in Section C (as it was not required to stabilize it further).



All dimensions in mm: Not to Scale: Symmetrical about longitudinal centreline

- A: Semi-circular duct 4 mm diameter
- B: Semi-circular duct 3.5 mm diameter
- C: Square duct 3.5 x 3.5 mm

Figure 6. Layout of open top package

116

117 The FBGs used in this work as the basis of the sensor system were manufactured using an
 118 excimer laser-based FBG-fabrication facility at City, University of London. Boron/Germanium
 119 co-doped fibres from Fibercore (PS1250/1500) were used as the photosensitive fibres in which was
 120 imprinted an interference pattern, created by using a phase mask, after exposure to light from a high
 121 power KrF excimer laser, operating in the ultra violet at 248 nm. During the inscription process, the
 122 laser source operated with a pulse energy of 10 mJ and a pulse frequency of 100 Hz. Different
 123 phase masks were used in order to manufacture FBG sensors, with different Bragg wavelengths,
 124 which then allowed ease of multiplexing (and thus the identification of an individual grating by its
 125 signature wavelength) when wavelength-division-multiplexing method was used to take multiple
 126 measurements. A plano-cylindrical lens with a focal length of 200 mm was placed in front of the
 127 laser allowing the laser beam to be focused into a thin line, with a width of approximately 0.5 mm

128 and length of around 8 mm. The laser beam was projected to the phase mask to create the required
 129 interference pattern which was subsequently imprinted to the photosensitive fibre which was placed
 130 close to the phase mask to modulate its core refractive index. In order to monitor closely the
 131 manufacturing process and control the reflectivity of the FBG fabricated, it was essential to monitor
 132 the FBG formation as it occurred during laser beam exposure by connecting it to a commercial
 133 interrogator system, Type *sm125* manufactured by Micron Optics, this being done using an external
 134 fiber. Figures 7 and 8 show photographs of the equipment used and the way the gratings are
 135 fabricated for use in this sensor system.

136 Testing of the quality and integrity of the packaged sensors that were developed for this
 137 application was done by mounting them on a steel beam and then subjecting them to a series of load
 138 cycles in the well-calibrated laboratory environment. This approach of using a steel beam had the
 139 key advantage that its behavior would be linearly elastic under repeated loads provided, of course,
 140 that stresses were kept within the elastic range (as was ensured). A square hollow section was
 141 chosen as this type has excellent resistance to both lateral torsional buckling and web buckling.
 142

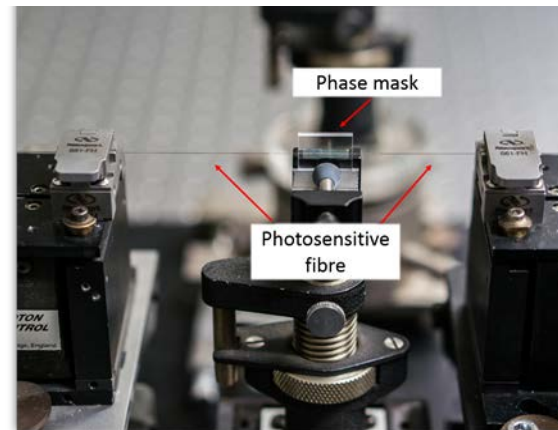
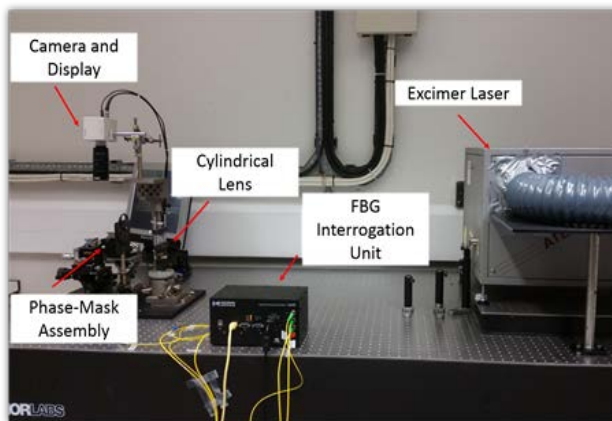


Figure 7. Basic configuration of FBG manufacturing **Figure 8.** Phase mask setup for FBG manufacturing

143 Thus the chosen test section for mounting the sensor package was a 60 mm x 60 mm square
 144 hollow section steel beam having a 3 mm wall thickness (i.e. a 60x60x3 SHS), which was mounted in
 145 a standard laboratory testing machine. The distance between the simple supports of the machine
 146 was 1500 mm and two point loads were applied using a spreader beam which gave a symmetrical
 147 four point loading arrangement. The constant moment zone (i.e. the distance between the two
 148 applied loads) was 500 mm, as is illustrated in Figure 9.

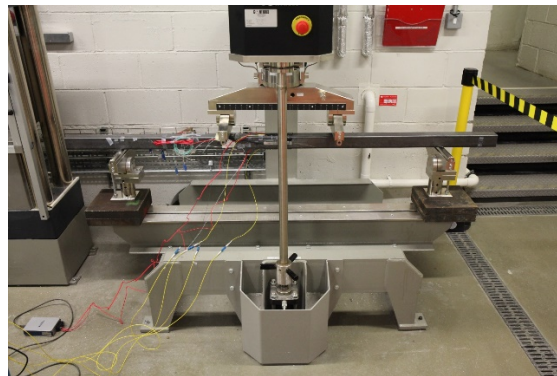


Figure 9. Test rig used in this work for assessment of the packaged sensors developed

149

150 The two open-top packages were glued to the mid-point of the beam i.e. at the center of the
151 constant moment zone and beside them a commercially sourced and packaged electric resistance
152 strain gauge (esrg) was glued to provide a simple calibration – this being 125 mm long, 13 mm wide
153 and 5 mm thick, with a Gauge Resistance of 120 ohm and a Gauge Factor of 2.1 (Type PML-120-2LJD
154 manufactured by Tokyo Measuring Instruments Lab). Duralco 4525-IP adhesive was used to bond
155 all the sensor types to the steel beam, particular care and attention being given to this operation in
156 view of the importance of achieving full strain transfer between the bonded surfaces. Prior to
157 mounting the packaged esrg sensor, a longitudinal groove was carefully cut in both the top and
158 bottom faces of the packaging material into each of which were glued three bare FBGs multiplexed
159 on a single fiber. Beside this packaged esrg, three bare FBGs, again multiplexed on a single fiber,
160 were glued directly onto the face of the steel beam. This was done to allow the output data from the
161 packaged FBGs to be benchmarked against all the other sensors (which then provided a high degree
162 of redundancy (as is needed for use in-the-field). Figure 10 shows a photograph of this sensor
163 arrangement used here.

164

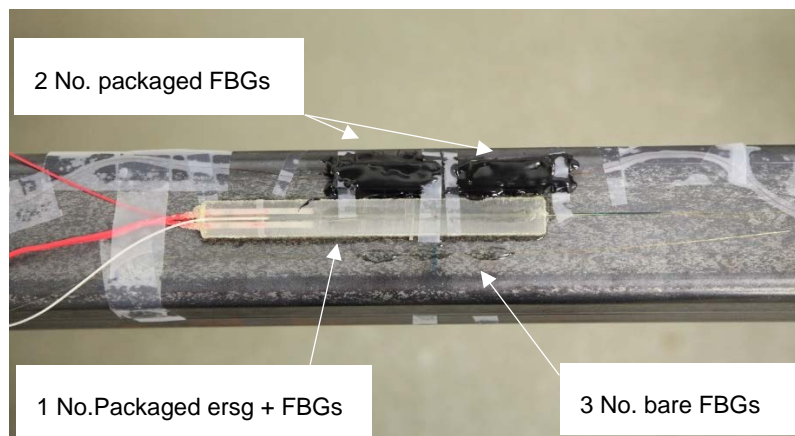
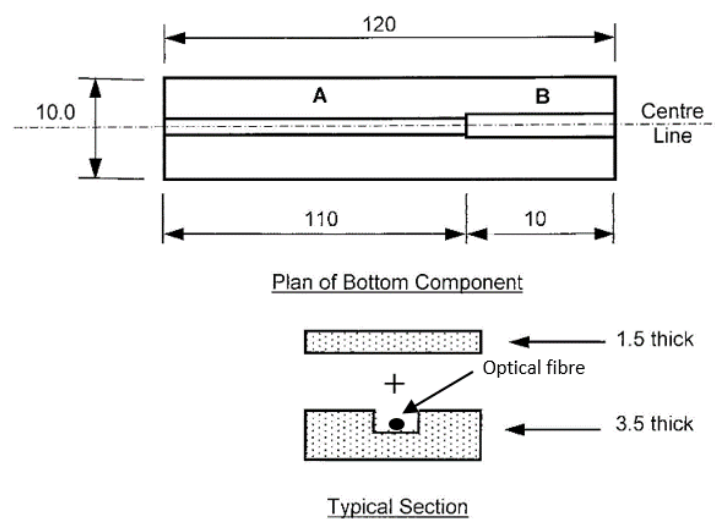


Figure 10. Detail of sensor layout on steel beam

165 To investigate the performance in detail, a series of load histories, representative of what would
166 be experienced in-the-field, was applied to the beam to test the performance of the sensor system
167 package under both cyclic and sustained loads. Data from the FBG-based sensors were collected
168 using a Micron Optics Type sm130 interrogator with a sampling frequency of 1 kHz and a
169 wavelength accuracy of ± 2 pm. This interrogator was chosen as it had 16 input channels, which
170 enabled FBG-based sensors which used similar wavelengths to be kept as separate channels in this
171 experiment, for ease of identification. Data from the esrg that was used for the cross-calibration
172 were collected using a standard laboratory instrument.

173 Following on from these tests, results from which are discussed in the next section, a more
174 sophisticated packaged sensor was designed and tested to allow for wider use in-the-field. The
175 new sensor had similar overall dimensions to the packaged esrg sensors considered and used earlier,
176 an approach which was designed to give confidence to users in industry when seeking to replace
177 ‘familiar’ devices by new technology. The essential novelty of the work lies in the approach taken
178 to 3D print sensor packages tailored to the specific need of the application and allow the
179 incorporation of as many FBG-based sensors as are required for the specific use of the sensor

180 package by industry. This allows the user to break away from the constraints of the use of
 181 conventional packaged esrgs. Since packaged esrgs are specifically designed for both surface
 182 mounting and embedment in concrete structures (without the need for bolted connections), it
 183 seemed sensible, for this exercise, to manufacture the new FBG-based sensor package to have similar
 184 dimensions and surface characteristics for easy comparisons to be made. This shows the versatility
 185 of the approach used. However, in other applications the sensor package could be designed to be
 186 completely different from that where esrgs are used and be lighter and more compact, or contain a
 187 larger number of sensors. Such flexibility in design with the FBGs, the 3D printing and an ability to
 188 meet the specific needs of the geometry and conditions of the site where the packaged device is to be
 189 used is a strength of this approach, described here for one such specific application. The device
 190 thus designed is shown in Figure 11, it being printed in two parts, with the dimensions given in the
 191 Figure. Here the package consisted of a *top* and a *bottom*, where these two parts were glued
 192 together after the installation of the FBGs that formed the sensor elements themselves. The device
 193 was made more robust as a result of this design, with a view for it being cast in a concrete beam and
 194 yet survive to read-out the strain data. To assist with this, a tough photopolymer resin, cured under
 195 UV light, was used which operated at a temperature between 40 to 50 °C. Curing lasted for one
 196 hour, and when tested the Young's modulus was 2.5 GPa. Again, Duralco 4525-IP resin was used
 197 to bond together the two halves of the package. Two FBGs were again installed in each package,
 198 mirroring the previous design. The FBG in Section A (to be used for strain measurement) was
 199 glued to the package with Duralco 4525-IP while the FBG in Section B (to be used for temperature
 200 measurement) was kept free by not being glued. Again, both FBGs were multiplexed onto a single
 201 fiber. Figure 12 shows the similarity in the dimensions of the commercial packaged esrg and the
 202 system created using the FBG sensors described (this being done to give user confidence in ease of
 203 *switching* between one technology and the other). The FBG-based sensor package was evaluated in
 204 the laboratory using a similar sensor layout and test procedure to that described above for the
 205 previous design.



All dimensions in mm: Not to Scale: Symmetrical about longitudinal centreline

A: Semi-elliptical duct 1 mm wide x 1.5 mm deep
 B: Square duct 3.5 x 3.5 mm

Figure 11. Layout of closed package

206

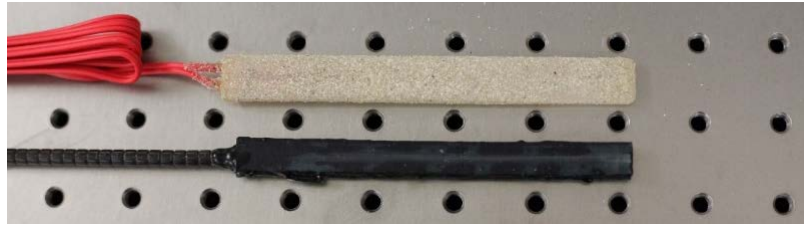


Figure 12. Packaged sensors: ersg top, FBG bottom

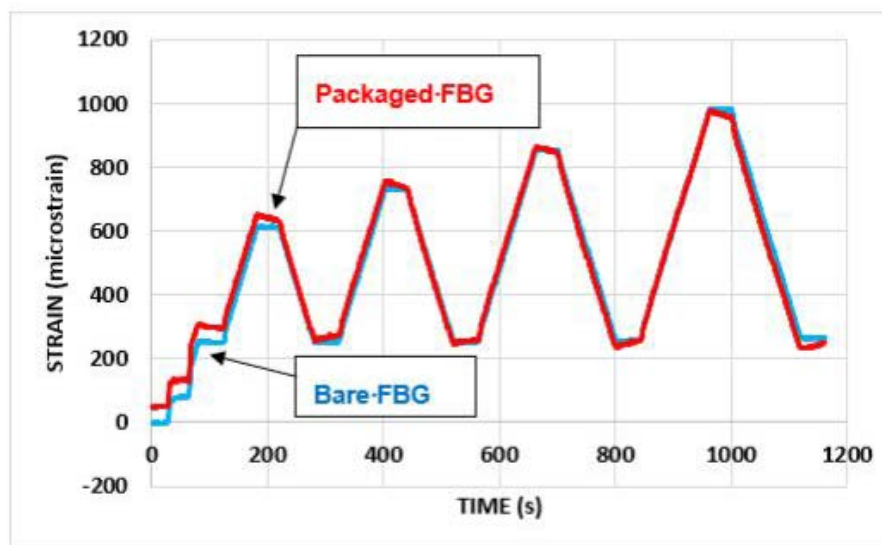
207 3. Results

208 3.1. Open Top Packages

209 Very similar responses were obtained from the packaged ersg and the *bare* FBGs that were
 210 evaluated and this was the case with all the load histories examined, with all showing excellent
 211 linearity and repeatability, with a total absence of creep. The temperature-monitoring FBG in the
 212 packaged sensor was stable throughout the tests, indicating that no significant temperature change
 213 had occurred (and thus no corrections for temperature were required).

214 Figures 13 and 14 show a comparison of the behaviour of the strain monitoring FBG when
 215 configured in the packaged sensor design, with that from the bare FBGs. Here Figure 13 shows
 216 results for successive increases in total load on the beam, while Figure 14 shows the behavior for
 217 repeated load cycles, with a total load of up to 5 kN being applied.

218 On first loading, the strain responses from the packaged sensor were greater than of those from
 219 the bare FBGs, possibly due to an initial *bedding-in* of the package on the steel beam, but this effect
 220 became less marked as the load was increased. The measurement of strains during both the loading
 221 and unloading was generally very similar, with the most noticeable feature of the results being the
 222 pronounced reduction in strain when loads were sustained (as is illustrated in Figure 14). This
 223 reduction was most likely caused by creep, but local slip or loss of adhesion between the package
 224 and the beam may also have occurred.



225 Figure 13. Open top package: response to load cycles to 5.0, 6.0, 7.0 & 8.0 kN (total load)

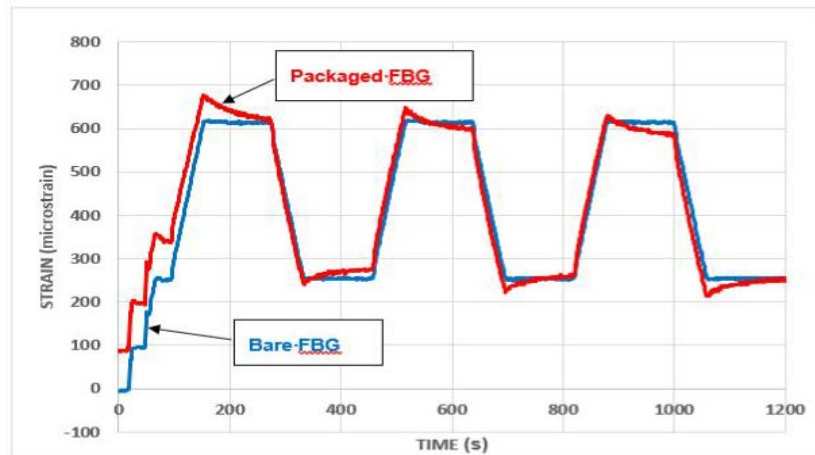


Figure 14: Open top package: repeated load cycles to 5.0 kN (total load)

226
227

228 3.2. Closed Top Package

229 The FBG used for temperature monitoring in the packaged sensor was again stable throughout
230 the tests (and thus no temperature corrections were needed).

231 Overall, as before, the response of the strain monitoring FBG in the packaged sensor was similar
232 to that for the bare FBGs. A typical comparison (in compression) is given in Figure 15. Using the
233 wavelength shift for the vertical axis emphasizes that the stiffness of the packaged FBG was
234 significantly less than that for the bare FBG (which is discussed in more detail in the next section).
235 Creep effects were also still present, although these were less pronounced than that which occurred
236 with the open top packages and also died away quite rapidly (as can be seen from Figure 16).

237
238

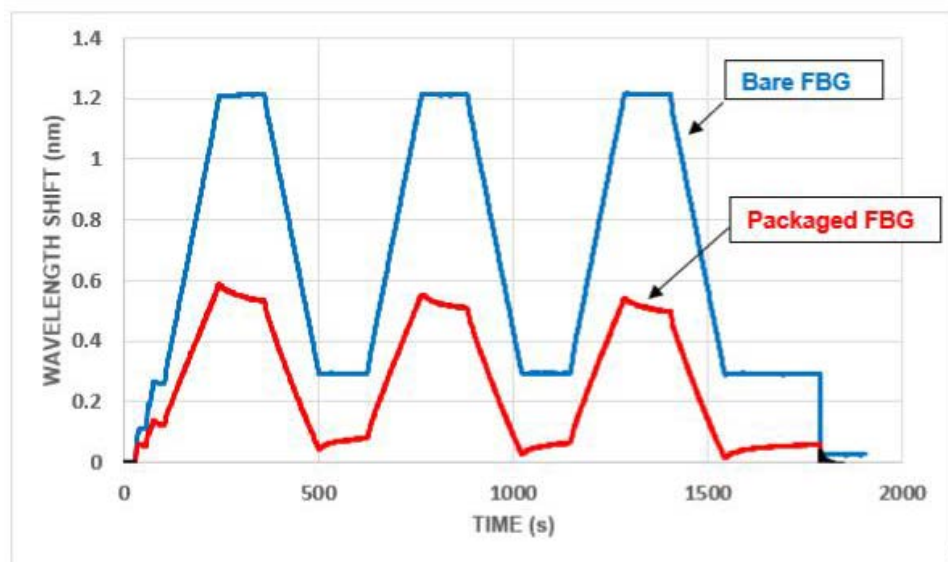
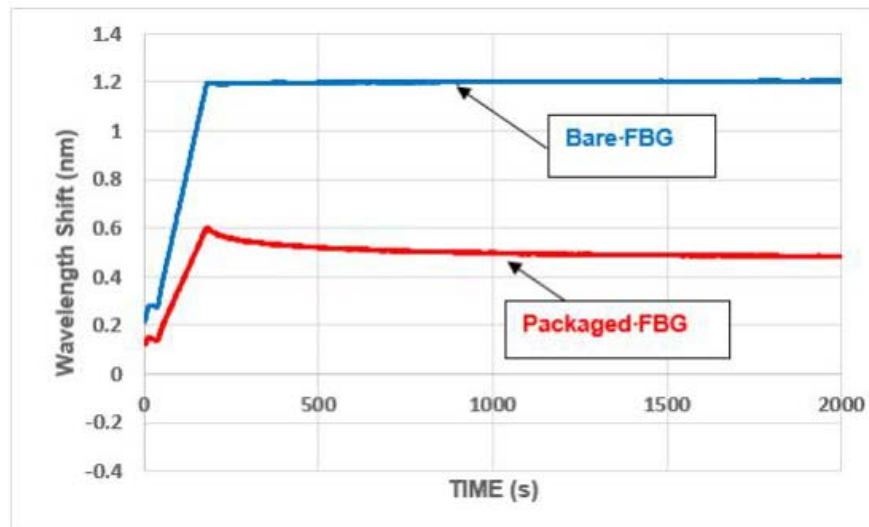


Figure 15. Closed top packages: repeated load cycles to 5.0 kN (total load)



hcx

Figure 16. Closed top package: creep behavior at 5.0 kN (total load)

239 4. Discussion

240 Strain sensitivities of the FBG-based packaged sensors were calculated by referencing them to the
 241 ersg results as a simple means of cross-calibration. The sensitivities of the FBG-based sensors used
 242 for temperature measurement were known from prior work but not explicitly calculated since, in
 243 view of the stable laboratory environment (in these tests temperature effects were minimal, and
 244 ignored), the focus was on the measured wavelength shifts which represent the underpinning sensor
 245 performance. Temperature calibration could be performed easily in future tests and would include
 246 controlled heating and cooling cycles. This would be particularly important for applications
 247 in-the-field where thermal effects are often unpredictable and thus accurate correction for
 248 temperature is needed. A specific example is the measurement of thermochemical effects during
 249 the period when concrete is curing. It is also recognised that polymer structures absorb water (i.e.
 250 swell) and the resulting effect on sensor performance will require some consideration.

251 The strain sensitivity of the open top packaged FBG-based sensors was found to be significantly
 252 lower (0.68 pm/microstrain) than that for the bare FBGs (1.13 pm/microstrain). This lower
 253 sensitivity is not unexpected when sensors are packaged and the low stiffness of the resin used for
 254 the packaging was most likely the cause of the creep problem. This does not represent a problem in
 255 use as the packaged sensor is then calibrated, rather than the bare FBG itself. The slightly lower
 256 sensitivity seen means that this packaged device can be used for all but the most sensitive of
 257 measurements desired.

258 The sensitivity of the closed top package was found to be 0.54 pm/microstrain in tension and
 259 0.36 pm/microstrain in compression. Bearing in mind that a stiffer resin had been used for this
 260 sensor, the reduction in stiffness and the continuing presence of creep were both somewhat
 261 disappointing but again the behavior and overall sensitivity of the packaged sensor was still
 262 considered to be encouraging for use in-the-field.

263 Thus, this slightly lower sensitivity, although undesirable, was not, in itself, seen as any real
 264 problem as the sensors of this type will be calibrated in advance of their use and the packaging
 265 conditions are consistent from sensor to sensor, thereby making the calibration predictable and

266 consistent from device to device. Consequently, these tests were deemed sufficiently encouraging
267 to justify further development work being undertaken.

268 It is recognized in the work described in this paper that this is just the first stage in the
269 development of inexpensive, easy-to-use packaged fiber optic sensors which are suitable for
270 commercial civil engineering applications and, given the packaged dimensions, to be direct
271 replacements for packaged esrgs. Thus, this early proof-of-concept work shows promise and gives
272 encouragement for further development work to be undertaken. Experience gained from the work
273 reported in this paper indicates that issues to be addressed further include the following:

- 274 • significantly reduce the mismatch between the stiffness of the packaging material of the sensors
275 and that of concrete or steel, which is the likely root cause of the creep problems. Possibilities
276 to overcome this include using PEEK (polyether ether ketone) or, perhaps more likely, ceramic
277 resins for the packaging, although it is important to keep in mind the need to control costs to
278 allow wider adoption of the sensor device. However, it is good to note that PEEK is not more
279 overly expensive compared with the resins used to date but using ceramics requires more
280 sophisticated hardware for the curing process. As often happens with engineering decisions,
281 optimizing the sensor requires a trade-off between performance and cost, but costs would have
282 to rise considerably before 3D-printed packages were as expensive as the currently available
283 commercial sensors. Additionally, reducing the thickness of the packaging is highly desirable
284 and may be assisted by encapsulating the FBGs in the packaging at the time of printing.
- 285 • perform durability tests of the package materials to assess resistance to an alkaline
286 environment, moisture and wear to allow their use in a wide variety of environments.
- 287 • ensure sensors perform the same in tension and in compression, maximize the sensitivities
288 (when compared to the figures achieved to date) and ensure that these are consistent in
289 performance between sensors of a similar type and size.
- 290 • ensure similar behaviour between sensors which are surface mounted and those which are
291 embedded.

292 Finally, an important aspect of the next stage will be to evaluate sensor performance under more
293 typical civil engineering conditions, such as embedment in reinforced concrete beams. Installation
294 of sensors in a concrete beam must always be undertaken very carefully to preserve the integrity of
295 the sensors and civil engineers are well experienced with this. Consequently, no additional
296 problems are anticipated when installing packaged FBG sensors compared with the established
297 packaged esrg sensors. Good performance is expected from the FBG packages and this will be
298 reported in due course.

299 5. Conclusions

300 A number of conclusions can be drawn from the positive outcomes of the above work, as
301 follows:

- 302 • a need for low cost packaged fibre optic sensors for strain measurement in civil engineering
303 applications has been identified and then met in the design reported, with potential for use in
304 monitoring reinforced concrete structures.
- 305 • sensor systems of that type have been effectively packaged (encapsulated) in resin using 3D
306 printing techniques, creating a low-cost and effective device for use in these applications which
307 has a consistent calibration and good sensitivity.

- 308 • ‘proof-of-concept’ laboratory testing has demonstrated the potential of the packaged sensors for
 309 strain measurement in civil engineering applications.
 310

311 **Author Contributions:** conceptualization, Banerji, Chikermane, Grattan, Scott, Sun, Vidakovic; methodology,
 312 Chikermane, Scott, Sun, Vidakovic; investigation, Chikermane, McKinley, Scott, Vidakovic; data curation, Scott,
 313 Vidakovic.; writing: Grattan, Scott, Vidakovic; project administration, Scott, Sun; funding acquisition, Banerji,
 314 Grattan.

315 **Funding:** This was a UKIERI-DST project (UKIERI-DST-201415-056) funded jointly by the Governments of the
 316 UK and India and the support given by this award is greatly appreciated.

317 **Acknowledgements:** The support given by the Royal Academy of Engineering and the George Daniels
 318 Educational Trust are both appreciated.

319 **Conflicts of Interest:** The authors declare no conflicts of interest.

320 References

- 321 1. Grattan, K.T.V. and Sun, T., (2000), Fiber Optic sensors technology: an overview, *Sensors and Actuators A:*
 322 *Physical*. Vol.82, no 1-3, pp. 44-61
- 323 2. Surre, F., Scott, R.H., Banerji, P., Basheer, P.A.M., Sun, T. and Grattan, K.T., (2012), Study of reliability of
 324 fibre Bragg grating fibre optic strain sensors for field-test applications. *Sensors and Actuators A: Physical*,
 325 185, pp.8-16.
- 326 3. Liang Fang, Tao Chen, Ruiya Li and Shihua Liu, (2016), Application of embedded fiber Bragg grating
 327 (FBG) sensors in monitoring health to 3D printing structures, *IEEE Sensors Journal*, 16(17), pp 6604-6610.
- 328 4. Liacouras, P.C., Grant, G.T., Choudhry, K., Strouse, G.F. and Ahmed, Z., (2015), Fiber Bragg gratings
 329 embedded in 3D printed scaffolds, *NCSLI Measure*, 10(2), pp 50-52
- 330 5. Canning, J., (2016), Drawing optical fibers from three dimensional printers, *Optics Letters*, 41(23), pp
 331 5551-5554
- 332 6. Zubel, M.G., Sugden, K., Webb, D.J., Saez-Rodriguez, D., Nielsen, K., and Bang O., (2016), Embedding
 333 silica and polymer fiber Bragg gratings (FBG) in plastic 3D-printed sensing patches, *Micro-Structured and*
 334 *Speciality Optical Fibers IV*, Proc of SPIE 9886 98860N-1
- 335 7. Thanh-Canh Huynh and Jeong-Tae Kim, (2017) FOS-based prestress force monitoring and temperature
 336 effect estimation in unbonded tendons of PSC girders, *Journal of Aerospace Engineering*, 30(2)
- 337 8. Moyo, P., Brownjohn, J.M., Suresh, R. and Tjin, S.C., (2005), Development of fiber Bragg grating sensors
 338 for monitoring civil infrastructure, *Engineering Structures*, 27(12), pp 1828-1834
- 339 9. Zheng, Z., Sun, X., and Lei, Y., (2009), Monitoring corrosion of reinforcement in concrete structures via
 340 fiber Bragg grating sensors, *Frontiers of Mechanical Engineering in China*, 4(3), pp 316-319
- 341 10. Nellen, P.M., Broennimann, R. and Sennhauser, U., (2000), Optical fiber Bragg gratings for structural
 342 monitoring in civil engineering, *Congress-International Association for Bridge and Structural Engineering*,
 343 IABSE, Sept 2000, pp 312-313
- 344 11. Matveenko, V.P., Shardakov, I.N., Voronkov, A.A., Kosheleva, N.A., Lobanov, D.S., Serovae, G.S.,
 345 Spaskova, E.M., and Shipunov, G.S., (2018), Measurement of strains by optical fiber Bragg grating sensors
 346 embedded into polymer composite material, *Structural Control and Health Monitoring*, 25(3), *John Wiley*,
 347 ISSN 1545-2255
- 348 12. Majumder, M., Gangopadhyay, T.K., Chakraborty, A.K., Dasgupta, K. and Bhattacharya, D.K., (2008),
 349 Fibre Bragg gratings in structural health monitoring—present status and applications. *Sensors and*
 350 *Actuators A: Physical*, 147(1), pp.150-164.
- 351 13. Grattan, S. K. T., Taylor, S. E., Basheer, P. M. A., Sun, T., & Grattan, K. T. V. (2011), Sensors systems,
 352 especially fibre optic sensors in structural monitoring applications in concrete: An overview. *Lecture Notes*
 353 *in Electrical Engineering*, 96, 359-425.
- 354 14. K.T.V.Grattan K.T.V and Meggitt B.T. (Eds), *Optical Fibre Sensor Technology, Volume 2: Devices and*
 355 *Technology*, Kluwer Academic Publishers, 2000
- 356 15. Banerji, P., Chikermane, S., Scott, R., Surre, F., Sun, T., Grattan, K. T. V., & Longthorne, J. (2014).
 357 Structural monitoring for asset management of railway bridges. *Proceedings of the Institution of Civil*
 358 *Engineers: Bridge Engineering*, 167(3), 157-169.
- 359 16. Wang Y, Vidakovic M, Scott RH, Wu Q, Sun T & Grattan KTV, (2017), Optical fibre sensor with 3D printed
 360 package configuration: a potential revolution of structural strain testing, *Mechanics of Structures and*
 361 *Materials: Advancements and Challenges*, Taylor & Francis Group, London

362



© 2019 by the authors. Submitted for possible open access publication under the terms and conditions of the Creative Commons Attribution (CC BY) license (<http://creativecommons.org/licenses/by/4.0/>).

363